Cureus Journal of Engineering
https://doi.org/10.7759/s44388-026-00374-2

Original Article

Development and Field Performance of a High-Visibility Thermoplastic Road Marking Formulation

Xiaotian Jiang [1, 2]

1. *Research Department, Guizhou Expressway Industry Co. Ltd., Guiyang, CHN*
2. *Research Department, Guizhou Highway Traffic Maintenance Technology Innovation Center, Guiyang, CHN*

Received: March 16, 2026 | Review began: March 26, 2026 | Review ended: September 18, 2026 | Published: November 17, 2026

© **Copyright** 2026
This is an open access article distributed under the terms of the Creative Commons Attribution License CC-BY 4.0., which permits unrestricted use, distribution, and reproduction in any medium, provided the original author and source are credited.

Abstract

Thermoplastic road marking coatings are composed of a resin binder, inorganic fillers, titanium dioxide pigment, glass beads, and functional additives. The proportioning of these components determines the mechanical durability, thermal stability, and optical performance of the coating, yet systematic formulation studies remain limited. This study developed a high-visibility thermoplastic road marking formulation through a single-factor experimental approach to address the common durability problems of thermal deformation and rapid retroreflectivity loss under heavy traffic and high-temperature conditions. The investigation quantitatively evaluated the effects of premixed glass bead dosage, the mass ratio of quartz sand to calcium carbonate filler, and titanium dioxide pigment content on the mechanical strength, thermal resistance, and optical performance of the coating. The experimental results demonstrated that a premixed glass bead content ranging from 31% to 33% provided the best combination of wear resistance and compressive strength. Regarding the filler composition, a quartz sand fraction of 6% to 7% formed a rigid skeletal network that effectively improved thermal deformation resistance and maintained compressive strength at 60°C. For optical performance, a rutile titanium dioxide dosage of 4.5% to 5.5% met the luminance factor requirements while avoiding the diminishing returns caused by particle agglomeration at higher concentrations. The optimized formulation, which employed a simplified additive system consisting solely of polyethylene wax and dioctyl phthalate plasticizer, was applied in a highway maintenance project with drop-on glass beads. Six months of field tracking showed that the initial retroreflectivity reached 481 $mcd \cdot m^{-2} \cdot lx^{-1}$ and stabilized at 342 $mcd \cdot m^{-2} \cdot lx^{-1}$, confirming that the formulation meets the durability requirements for high-traffic highways. The findings demonstrate that careful proportioning of functional components can balance performance and cost without relying on complex multi-additive systems.

Categories: Materials Engineering, Transportation Engineering, Polymer Science and Engineering

Keywords: thermoplastic road marking, retroreflectivity, compressive strength, wear resistance, field validation

Introduction

Road markings guide drivers and organize traffic flow, contributing to nighttime and wet-weather safety [1-5]. Among available marking materials such as solvent-based paints, waterborne coatings, two-component coatings, and thermoplastic coatings, thermoplastics dominate highway applications. They cure within minutes, allowing lane reopening shortly after application, and they adhere firmly to pavement and resist abrasion from tire contact [6-8]. Solvent-based paints are restricted by volatile organic compounds regulations. Waterborne coatings dry slowly in humid conditions and are rarely used on high-traffic highways. Two-component coatings offer good durability but require mixing at the job site and careful timing control.

A typical thermoplastic road marking formulation comprises 15% to 20% thermoplastic resin binder, 35% to 45% inorganic fillers (calcium carbonate and quartz sand), 4% to 8% rutile titanium dioxide pigment, 30% to 35% premixed glass beads, and 1% to 3% functional additives (plasticizers and waxes). The resin binder serves as the continuous phase providing adhesion to the pavement. The fillers contribute mechanical strength and thermal stability. The titanium dioxide pigment provides whiteness and hiding power. The premixed glass beads, together with drop-on glass beads applied during construction, enable nighttime retroreflectivity. The additives regulate melt flow and low-temperature flexibility. Understanding the function and proportioning of each component is a prerequisite for systematic formulation optimization.

Despite the widespread use of thermoplastics, rising traffic volumes, heavier axle loads, and more frequent extreme heat events are increasingly exposing the limitations of traditional formulations. Two primary degradation modes have been identified in recent field investigations [9,10]. First, the polymer matrix softens under high pavement temperatures, leading to deformation and rutting of the marking. Second, markings often exhibit high initial retroreflectivity that deteriorates rapidly during the first few months of service. Contractors frequently rely heavily on drop-on glass beads to pass initial inspections immediately after application, while overlooking the long-term contribution of premixed beads. Once the surface layer of drop-on beads is worn away by traffic, few premixed beads remain to sustain optical performance, causing retroreflectivity to drop sharply within three to four months.

Reformulating thermoplastics to achieve an optimal balance among mechanical strength, thermal resistance, and optical durability has therefore become an urgent task. Recent research efforts have focused on modifying individual components to enhance performance, such as improving interfacial bonding between the resin matrix and glass beads through surface treatments. Zhao et al. [10] developed a service life prediction model for thermoplastics based on field retroreflectivity decay patterns on expressways. Quan et al. [11] demonstrated that nano-SiO_2 and nano-TiO_2 modifications can improve the durability of tunnel road markings, while Wang et al. [12] investigated the effects of glass bead size and surface treatment on bonding performance.

Recent studies have addressed the durability of thermoplastic road markings from multiple perspectives. Eren et al. [13] reported that glass-based fillers in light-colored pavement surfaces exhibit an optimal dosage range, beyond which reflection performance declines due to non-uniform dispersion. Lu et al. [14] investigated the technical performance and workability of hot-melting road marking materials for high-altitude areas. Mirabedini et al. [15] applied mixture experimental design to optimize the formulation and performance of thermoplastic road markings, demonstrating the feasibility of statistical approaches in formulation development. Despite these advances, systematic studies on how the proportioning of multiple functional components collectively governs the mechanical, thermal, and optical performance of thermoplastic markings remain scarce.

However, at the formulation level, many commercial products still rely on complex additive packages that combine plasticizers, anti-settling agents, toughners, and other functional additives simultaneously and often excessively. While intended to balance multiple properties, this approach increases material costs, risks phase incompatibility among additives, and complicates quality control during production. More fundamentally, systematic studies on how the proportioning of fillers, pigments, and reflective agents collectively governs mechanical, thermal, and optical performance remain scarce. Without such knowledge, formulations risk either underperforming in critical properties or relying on costly additive overuse. Recent reviews have also highlighted that the selection of marking materials involves not only performance considerations but also environmental and economic trade-offs that are rarely addressed in formulation studies [8,16].

To address this gap, the present study systematically investigates how the proportioning of key components governs coating performance. The components examined include premixed glass beads, the quartz sand to calcium carbonate ratio, titanium dioxide pigment, and functional additives. The performance metrics evaluated are wear resistance, thermal deformation resistance, flowability, and luminance factor. A single-factor experimental design was adopted to isolate and quantify the contribution of each component. Based on the parametric analysis, a formulation with a

simplified additive system was developed to balance performance and material cost. The optimized formulation was then applied in a highway maintenance project with a double-drop technique for glass bead application, and its retroreflectivity was tracked over six months to validate long-term field performance.

Materials And Methods

Raw materials and quality specifications

Thermoplastic road marking materials are multicomponent polymer matrix composites formulated from five essential ingredient categories. A thermoplastic resin binder serves as the continuous phase to provide adhesion to the pavement substrate. Functional fillers, including heavy calcium carbonate and quartz sand, are incorporated to confer mechanical strength, enhance thermal stability, and control production costs. Pigments, specifically rutile titanium dioxide, are added to achieve the required chromaticity and hiding power. Hiding power refers to the ability of a pigment to obscure the underlying surface color, which is essential for ensuring that the marking appears uniformly white and highly visible against the dark pavement background. Retroreflective elements are essential for nighttime visibility and are typically implemented as a dual-bead system. Premixed glass beads are blended into the coating to maintain long-term retroreflectivity as the marking wears, whereas drop-on glass beads are applied onto the wet surface during construction to deliver immediate initial luminance. Minor functional additives are used to regulate melt rheology and low-temperature flexibility.

To ensure the reliability of the experimental data and the long-term durability of the final composite, rigorous screening of the technical specifications for all raw materials was conducted. The primary raw materials and their required quality specifications are summarized in Table *1*.

Material Category	Test Item	Technical Requirement	Selected Material
Resin binder	Softening point (°C)	≥100	C5 aliphatic petroleum resin
Fillers	Whiteness (%)	≥90	325-mesh heavy calcium carbonate, high-purity quartz sand
Pigment	Crystal phase	Rutile phase	Rutile titanium dioxide
Reflective material	Refractive index	≥1.5	Premixed glass beads
	Roundness rate (%)	≥80	

TABLE 1: Raw materials and technical requirements

The softening point of the resin binder, measured at ≥100 °C, ensures that the coating maintains dimensional stability under high summer pavement temperatures without excessive softening or flow. The whiteness requirement of ≥90% for fillers guarantees that the calcium carbonate and quartz sand do not introduce discoloration that would compromise the final marking's brightness. The rutile crystal phase of titanium dioxide is specified because it provides superior hiding power and ultraviolet resistance compared to the anatase phase, which is prone to weather-induced degradation. For the reflective materials, the refractive index of at least 1.5 ensures that the glass beads can effectively refract and reflect incident light back toward the driver. The roundness rate of no less than 80% ensures that the beads are sufficiently spherical to provide consistent retroreflection and to disperse uniformly within the polymer matrix.

A high-performance C5 aliphatic petroleum resin was selected as the film-forming binder due to its excellent tackifying properties, thermal stability, and superior melt rheology behavior [17]. C5 aliphatic petroleum resins are hydrocarbon resins derived from C5 fractions of petroleum cracking, characterized by their light color, good thermal stability, and compatibility with various polymers and waxes commonly used in road marking formulations. For the pigmentation system, the conventional anatase titanium dioxide, which is prone to weather-induced degradation, was entirely replaced by the rutile phase titanium dioxide. The rutile crystalline structure possesses a higher refractive index and tighter atomic packing, thereby ensuring exceptional hiding power, whiteness, and ultraviolet aging resistance under prolonged outdoor exposure [18,19].

The composite filler comprised 325-mesh heavy calcium carbonate to provide bulk volume and fundamental compressive strength, along with high-purity quartz sand to enhance the rigid skeletal structure and thermal resistance. Furthermore, premixed glass beads with a high roundness rate of no less than 80% and a refractive index of at least 1.5 were utilized to guarantee consistent retroreflective performance after the initial surface beads wore off.

Experimental methods and parametric design

All core testing protocols were conducted in strict accordance with the Chinese transportation industry standard for pavement marking coatings, JT/T 280-2022, which specifies rigorous technical requirements for high-performance thermoplastic materials. This standard is comparable in scope to EN 1871 for road marking materials, covering laboratory tests for mechanical, thermal, and optical properties.

To evaluate the mechanical endurance of the coating under varying environmental conditions, compressive strength was tested at both 23 °C and 60 °C. The standard 23 °C test reflects typical service conditions, while the 60 °C test simulates extreme summer pavement temperatures to verify that the material does not fail under thermal stress. Compressive strength was measured using cylindrical specimens of 20 mm diameter and 20 mm height. Testing was conducted at both 23°C and 60°C at a loading rate of 5 mm/min. Each reported value is the average of five replicate specimens.

The long-term durability of the marking against tire friction was assessed by measuring the wear value, defined as the mass loss of a standardized coating sample after being subjected to controlled abrasive cycles. Wear resistance was evaluated using an abrasion tester with a standard abrasive wheel under a load of 1 kg for 200 cycles. Wear value is defined as the mass loss in milligrams (mg), measured with a balance accurate to 0.1 mg.

Thermal deformation resistance was evaluated to ensure the dimensional stability of the coating, confirming that it will not soften, flow, or develop ruts when exposed to high environmental heat. Thermal deformation resistance was determined by placing specimens of 100 mm × 100 mm × 5 mm in an oven at 60°C under a specified load for 2 hours. The result is expressed as the percentage of the original dimension retained.

Flowability, measured during the molten state, was tested to guarantee that the material possesses the appropriate melt rheology for smooth extrusion and leveling by application equipment; it is expressed as the spreading area per unit mass of the molten material.

Furthermore, the overall whiteness and daytime visibility of the marking, which depend highly on pigment hiding power, were quantitatively determined by measuring the luminance factor. The luminance factor is the ratio of the luminance of the test surface to that of a perfectly diffuse white reference surface under the same illumination conditions, expressed as a percentage.

To provide a clear benchmark for evaluating the formulation's performance, the technical requirements for the core experimental indicators as stipulated by JT/T 280-2022 are summarized in Table *2*. The test procedures specified in this standard are analogous to those described in EN 1871 for the physical properties of road marking materials.

Performance Indicator	Technical Requirement	Comparable International Standard
Compressive strength at 23°C	≥12.0 MPa	EN 1871

Compressive strength at 60°C	≥2.0 MPa	EN 1871
Wear value	≤80 mg	EN 1871
Thermal deformation resistance	≥90%	EN 1871
Flowability	85-95 mm^2/g	EN 1871
Luminance factor	≥ 80%	ASTM D4960

TABLE 2: Technical requirements for core performance indicators of thermoplastic marking

Beyond mechanical and thermal properties, practical construction workability and optical performance were also rigorously examined. To systematically decouple and evaluate the influence of individual components, a parametric sensitivity design was adopted. A common flaw in traditional formulations is the excessive use of complex, multicomponent additives, such as specific chemical waxes, ethylene-vinyl acetate copolymer, and coloring agents, which can introduce severe cross-interference in performance testing. Therefore, from the outset of this study, a streamlined baseline additive package consisting solely of a plasticizer (dioctyl phthalate, which was fixed at 0.7%) and polyethylene wax (which was fixed at 0.8%) was established. Dioctyl phthalate, abbreviated as DOP, functions as a plasticizer to provide low-temperature flexibility and adequate plasticization of the resin matrix. With the C5 petroleum resin also maintained constant at approximately 16% to ensure a stable viscoelastic matrix, controlled variable gradients were introduced sequentially to investigate three primary compositional factors.

First, the effect of the reflective material was assessed by varying the premixed glass bead dosage from 30% to 35%. Second, the influence of the filler system was evaluated by adjusting the total filler content alongside the specific mass ratio of quartz sand to calcium carbonate. Finally, the impact of the pigment on optical properties was determined by modifying the rutile titanium dioxide content. Each set of gradient experiments was executed under the strict premise of keeping all other variables constant. This methodical approach enabled a precise and quantitative determination of how each single formulation parameter governs the macroscopic mechanical, thermal, and optical properties of the marking material.

Results And Discussion

Effect of glass bead dosage on road marking coating's performance

Glass beads act as the core functional fillers providing necessary nighttime retroreflectivity. To explore the optimal dosage limits, a series of gradient tests were conducted with the premixed glass bead content ranging from 30% to 35%. During these tests, the titanium dioxide content was fixed at 5% and quartz sand at 6.5%. The calcium carbonate content was correspondingly adjusted to balance the total mass. The experimental results are presented in Table *3*.

Formulation Code	Glass Beads (%)	Compressive Strength at 23°C (MPa)	Compressive Strength at 60°C (MPa)	Wear Value (mg)	Flowability (mm^2/g)
G1	30	23.9	2.12	75.2	92.8
G2	31	24.3	2.34	73.1	93.7

G3	32	24.1	2.55	71.8	94.8
G4	33	25.9	2.68	69.2	93
G5	34	24.8	2.51	67.5	89.6
G6	35	24.2	2.38	65.2	90

TABLE 3: Effect of glass bead content on road marking coating's performance

As shown in Table *3*, when the glass bead content increased from 30% to 35%, the flowability remained relatively stable, fluctuating only slightly between 89.6 mm^2/g and 94.8 mm^2/g. This stability is consistent with the known rheological behavior of spherical fillers in polymer melts. Due to their low aspect ratio and minimal interparticle friction, spherical particles generally cause less disruption to flow than irregularly shaped fillers [20,21]. Thus, within this range, adding glass beads does not compromise construction workability.

To further study the macroscopic mechanical evolution driven by the glass beads, the trends of wear value and compressive strength at 60°C are visually plotted in Figure *1*. The wear value, measured in milligrams (mg), represents the mass loss of the coating sample after abrasive cycling. The compressive strength, measured in megapascals (MPa), indicates the maximum stress the material can withstand at elevated temperature.

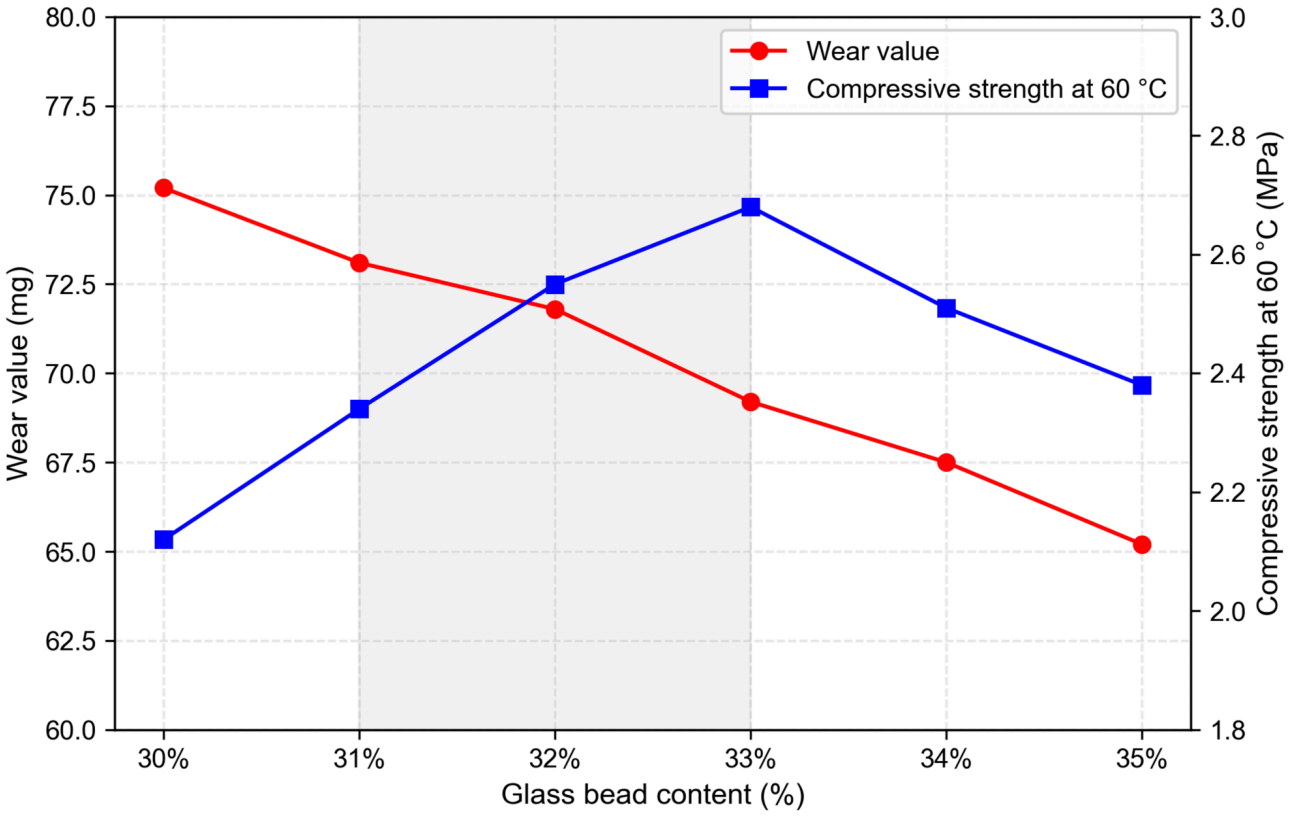


FIGURE 1: Effect of glass bead content on the wear value and compressive strength at 60°C of the road marking coating

The curves in Figure *1* reveal two distinct mechanical behaviors. First, the wear value exhibits a continuous and steady downward trend, dropping from 75.2 mg to 65.2 mg. This reduction signifies a marked improvement in the wear resistance of the coating. Because glass beads possess a high surface hardness, their appropriate incorporation allows these spherical particles to form a solid anti-wear skeleton within the continuous polymer matrix.

The compressive strength at 60 ℃ demonstrates a clear parabolic trend. The strength initially rises alongside the glass bead content, reaching a distinct peak of 2.68 MPa at a dosage of 33%. This initial enhancement is attributed to the rigid structural support provided by the beads resisting thermal softening. However, as the dosage exceeds 33%, the high-temperature compressive strength begins to gradually decline. This decline occurs because an excessively high volume of rigid inorganic particles disrupts the continuity of the viscoelastic matrix. Consequently, the petroleum resin fails to completely encapsulate the excess beads, which leads to weak interfacial binding forces and a deterioration of the overall structural integrity under thermal and mechanical stress.

By comprehensively balancing the requirements for high-temperature compressive strength, wear resistance, and economic cost, the optimal dosage range for premixed glass beads should be controlled between 31% and 33%. The best overall performance was achieved at 33% glass bead content, corresponding to the peak compressive strength. This optimal range is highlighted as the shaded target zone in Figure *1*.

Effect of filler on road marking coating's performance

The inorganic filler plays a vital role in reducing production costs and determining both the mechanical strength and thermal stability of the coating. In this experimental series, the glass bead content was fixed at 32% and titanium dioxide at 5%. The study investigated how the specific mass ratio of quartz sand to calcium carbonate affects the material properties under a controlled total filler content which was approximately 44%. The test results are detailed in Table *4*.

Formulation Code	Quartz Sand (%)	Calcium Carbonate (%)	Total Filler (%)	Compressive Strength at 60℃ (MPa)	Wear Value (mg)	Thermal Deformation (%)
F1	5	35	40	2.1	75.2	92.5
F2	5.5	36.5	42	2.3	72.5	92.2
F3	6	37.5	43.5	2.55	68.9	93
F4	6.5	37.5	44	2.8	65.4	93.8
F5	7	37	44	2.75	64.2	94.1
F6	7.5	36.5	44	2.65	63.5	95.5

TABLE 4: Effect of filler composition on road marking's coating performance

To illustrate the high-temperature mechanical evolution governed by the quartz sand fraction, the trends of compressive strength at 60℃ and thermal deformation resistance are plotted in Figure *2*. Thermal deformation resistance is defined as the percentage of the original specimen dimension retained after exposure to elevated temperature under a specified load.

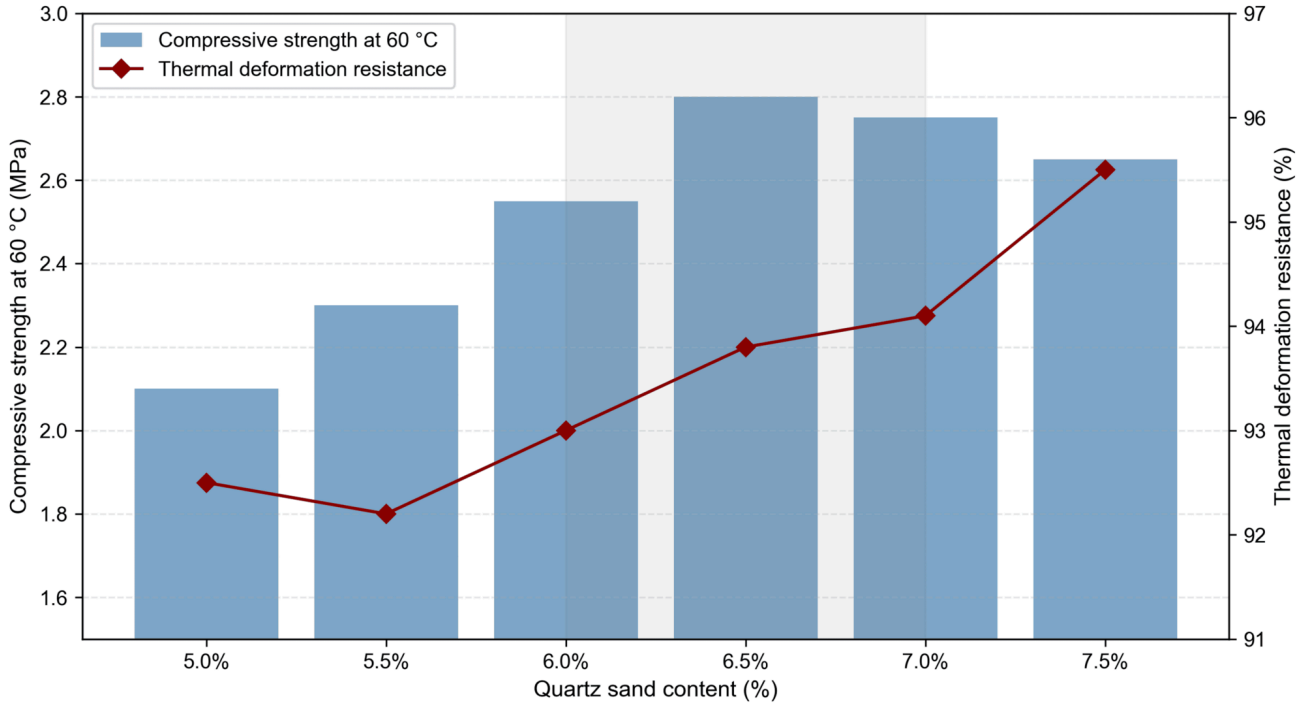


FIGURE 2: Effect of quartz sand content on the compressive strength at 60°C and thermal deformation resistance

The test data reveals that the composition of the filler exerts a significant impact on high-temperature resistance. As shown in the bar chart of Figure *2*, the compressive strength at 60°C rises sharply as the quartz sand content increases from 5.0%, reaching a peak of 2.86 MPa at a dosage of 6.5%. It then maintains a highly stable level at 7.0% before showing a slight decline at 7.5%. Concurrently, the line graph indicates that the thermal deformation resistance steadily improves, exceeding 94% when the quartz sand reaches the 6.5% to 7.0% range.

This synergistic enhancement of mechanical and thermal properties can be primarily explained by the distinct physical characteristics of the filler particles. Conventional heavy calcium carbonate consists of relatively soft, fine powders that are prone to yielding under high heat and pressure. In contrast, quartz sand provides exceptional Mohs hardness and inherent thermal stability. Within the composite matrix, the introduction of an appropriate amount of these rigid sand particles creates a robust interlocking structural network. The coarse quartz grains act as a rigid skeleton, while the finer calcium carbonate particles effectively fill the spatial voids between them. This well-graded filler packing greatly restricts the mobility of the softened petroleum resin matrix under extreme high summer pavement temperatures.

However, continuing to increase the quartz sand beyond 7.0% leads to excessive accumulation of rigid components. This causes a minor decline in high-temperature compressive strength due to the increased brittleness of the mixture and insufficient resin wetting. Based on these mechanical trends, the optimal internal filler proportion lies within a quartz sand fraction of 6.0% to 7.0%, paired with a calcium carbonate fraction of 36.5% to 38.0%. The best balance of compressive strength and thermal deformation resistance was achieved at 6.5% quartz sand content.

Effect of titanium dioxide dosage on optical performance of road marking

Rutile titanium dioxide acts as the primary white pigment, providing excellent chromaticity and hiding power for the road markings. The luminance factor, which is the ratio of the luminance of the test surface to that of a perfectly diffuse white reference surface under the same illumination, is the key parameter used to evaluate whiteness and daytime visibility. With the glass bead content fixed at 32% and the total filler content maintained at approximately 44%, the

titanium dioxide dosage was adjusted systematically from 4.0% to 7.0%. A portable spectrophotometer was utilized to measure the corresponding luminance factor of the resulting coatings. The experimental results are summarized in Table *5*.

Formulation Code	Titanium Dioxide (%)	Luminance Factor (%)
P1	4	77.5
P2	4.5	80.1
P3	5	83.2
P4	5.5	83.6
P5	6	84.1
P6	6.5	84.5
P7	7	84.7

TABLE 5: Effect of titanium dioxide dosage on road marking's coating performance

To better visualize the relationship between the pigment concentration and the macroscopic optical performance, the luminance factor data are plotted in Figure *3*. All data presented in this section represent initial performance measured on freshly prepared samples immediately after complete curing, with an age of approximately 48 hours from preparation to testing, to ensure consistent baseline conditions before any service exposure.

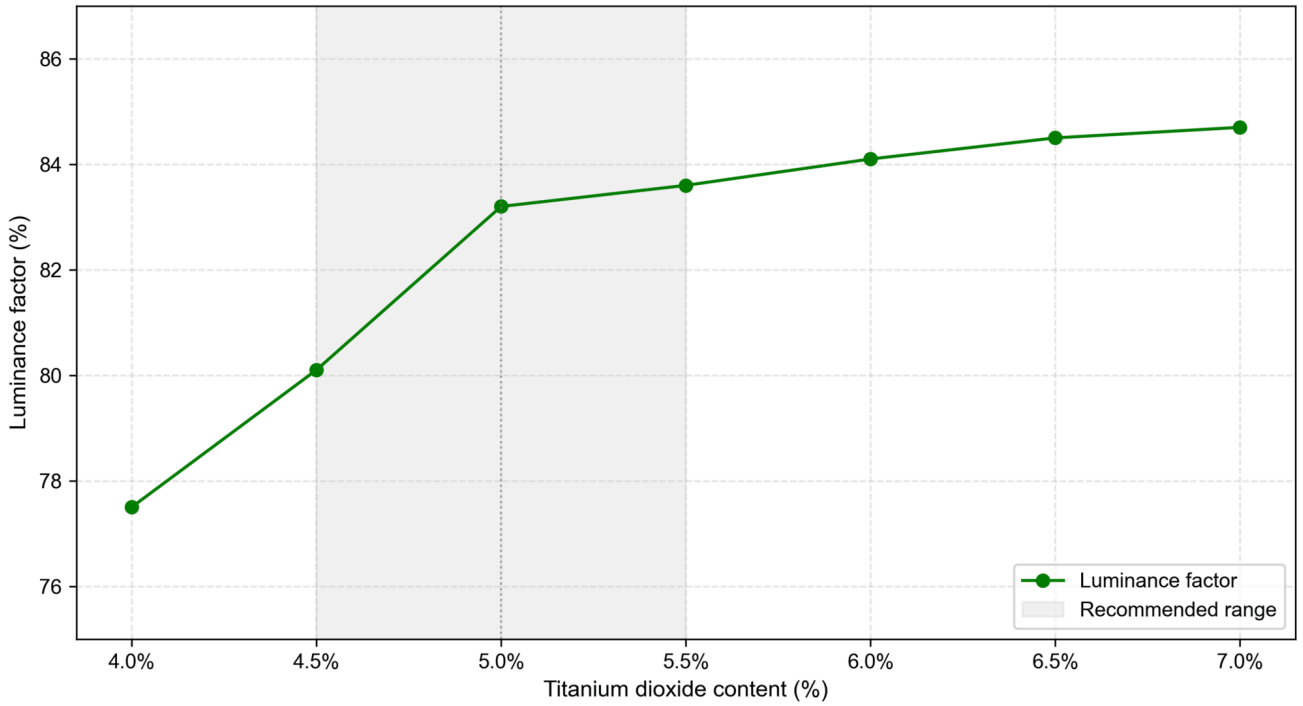


FIGURE 3: Effect of titanium dioxide content on the luminance factor

The saturation curve presented in Figure *3* indicates that the optical enhancement driven by titanium dioxide exhibits a pronounced marginal effect. During the initial phase, when the dosage increases from 4.0% to 5.0%, the curve displays a steep slope. The luminance factor jumps significantly from 77.5% to 83.2%, which fully meets and exceeds the standard requirements for high-visibility markings. However, as the dosage continues to increase beyond 5.5%, the curve transitions into a distinct plateau phase, where the growth rate of the luminance factor becomes extremely flat.

There is a saturation limit for the distribution of titanium dioxide particles within the polymer matrix. In the lower dosage range, the pigment particles are well dispersed, allowing each individual crystal to efficiently refract and scatter incident light. However, when the concentration becomes excessively high, the spatial distance between adjacent particles shortens significantly. This proximity inevitably leads to physical agglomeration and the overlapping of light scattering centers. Consequently, the light scattering efficiency of individual particles dramatically declines, rendering any further pigment addition optically redundant.

Considering both the saturation of the optical benefits and the high economic cost of the rutile pigment, the recommended dosage of titanium dioxide should be strictly controlled between 4.5% and 5.5%. The optimal dosage for balancing cost and optical performance is approximately 5.0%, where the luminance factor has already reached 83.2%, exceeding the standard requirement of 80% without entering the plateau of diminishing returns. This optimized range is highlighted by the shaded area in Figure *3*.

Recommended formulation

As detailed in the experimental design, to avoid phase incompatibility and cross-interference caused by traditional multi-component additive systems, this study adopted a streamlined additive strategy comprising only a plasticizer and polyethylene wax throughout the parametric testing. After the optimal skeletal framework of the primary components was established, final micro-adjustments were made to this streamlined additive system to secure the optimal balance between construction workability and long-term durability.

In this refined system, DOP functions to provide fundamental low-temperature flexibility and adequate plasticization. However, excessive DOP can drastically lower the softening point, leading to summer deformation. Thus, its dosage must be strictly confined to 0.5% to 1.0%. Conversely, polyethylene wax serves as an excellent bi-functional rheology modifier. It significantly improves melt flow behavior during high-temperature extrusion and provides robust anti-settling properties for dense particles. To prevent coating embrittlement, the optimal dosage range for polyethylene wax is determined to be 0.5% to 1.5%.

By comprehensively integrating the outcomes of the mechanical endurance, optical longevity, and thermal stability evaluations, alongside production economics, the recommended optimal dosage ranges for the finalized high-visibility thermoplastic road marking formulation are summarized in Table *6*.

Component Category	Material Name	Recommended Dosage Range (%)
Binder	C5 petroleum resin	15–18
Pigment	Rutile titanium dioxide	4.5–5.5
Reflective material	Premixed glass beads	31–33
Fillers	High-purity quartz sand	6–7
	Heavy calcium carbonate	36.5–38
Additives	DOP	0.5–1
	Polyethylene wax	0.5–1.5

TABLE 6: Recommended dosage ranges for thermoplastic marking formulation

Engineering application verification

Road Marking Application

To verify the practical reliability of the experimental findings, the recommended optimized formulation was applied in a real-world maintenance project on the G7611 Duxiang Expressway in Guizhou Province, China. The selected test section is a standard divided dual-carriageway highway with four lanes. During construction, the ambient temperature was stable between 20 °C and 24 °C, and the pavement surface remained entirely dry. To ensure that the polyethylene wax and resin matrix melted homogeneously while preventing the titanium dioxide from yellowing and the glass beads from settling prematurely, the extrusion temperature of the application equipment was strictly controlled between 200°C and 220°C. The on-site application process is shown in Figure *4*.



FIGURE 4: Application of thermoplastic road marking

How to cite this article:
Jiang X (November 17, 2026) Development and Field Performance of a High-Visibility Thermoplastic Road Marking Formulation. Cureus J Eng 3 : es44388-026-00374-2. DOI https://doi.org/10.7759/s44388-026-00374-2

In thermoplastic marking applications, premixed glass beads primarily govern long-term retroreflectivity after the surface matrix wears away. Conversely, the initial high-visibility performance depends heavily on the surface application of drop-on glass beads. These drop-on beads remain exposed on the uppermost layer of the marking and immediately refract and reflect vehicle headlight beams. To achieve superior nighttime and wet-night visibility, this engineering project utilized a total drop-on glass bead application rate of 600 g/m^2 implemented through a double-drop application technique.

First, large-diameter glass beads ranging from 850 μm to 1700 μm were applied at a rate of no less than 0.3 kg/m^2. This size range is consistent with the rain-enhanced glass bead category specified in GB/T 24722-2020 for special wet-night applications, where larger particles protrude above water films on wet pavement to ensure reliable retroreflectivity during rainy nights. These large beads are typically used in combination with conventional beads and should not exceed 30% of the total bead application to maintain daytime visibility. Immediately following this, medium-to-small glass beads ranging from 425 μm to 850 μm were applied at an equal rate of no less than 0.3 kg/m^2. These smaller beads efficiently fill the spatial gaps between the larger beads, creating a dense and continuous retroreflective surface. Throughout this dual-dispersion process, application uniformity was strictly monitored. By leveraging the viscosity and surface tension of the molten coating, the embedment depth of each drop-on bead was controlled precisely at 50% to 60% of its diameter. This specific embedment ratio represents the optimal optical position, preventing premature detachment while maximizing the effective retroreflective area. The appearance of the freshly applied road marking is shown in Figure *5*. Furthermore, Figure *6* provides a microscopic close-up view verifying the dense spatial packing and the 50% to 60% embedment depth achieved by the double-drop technique.

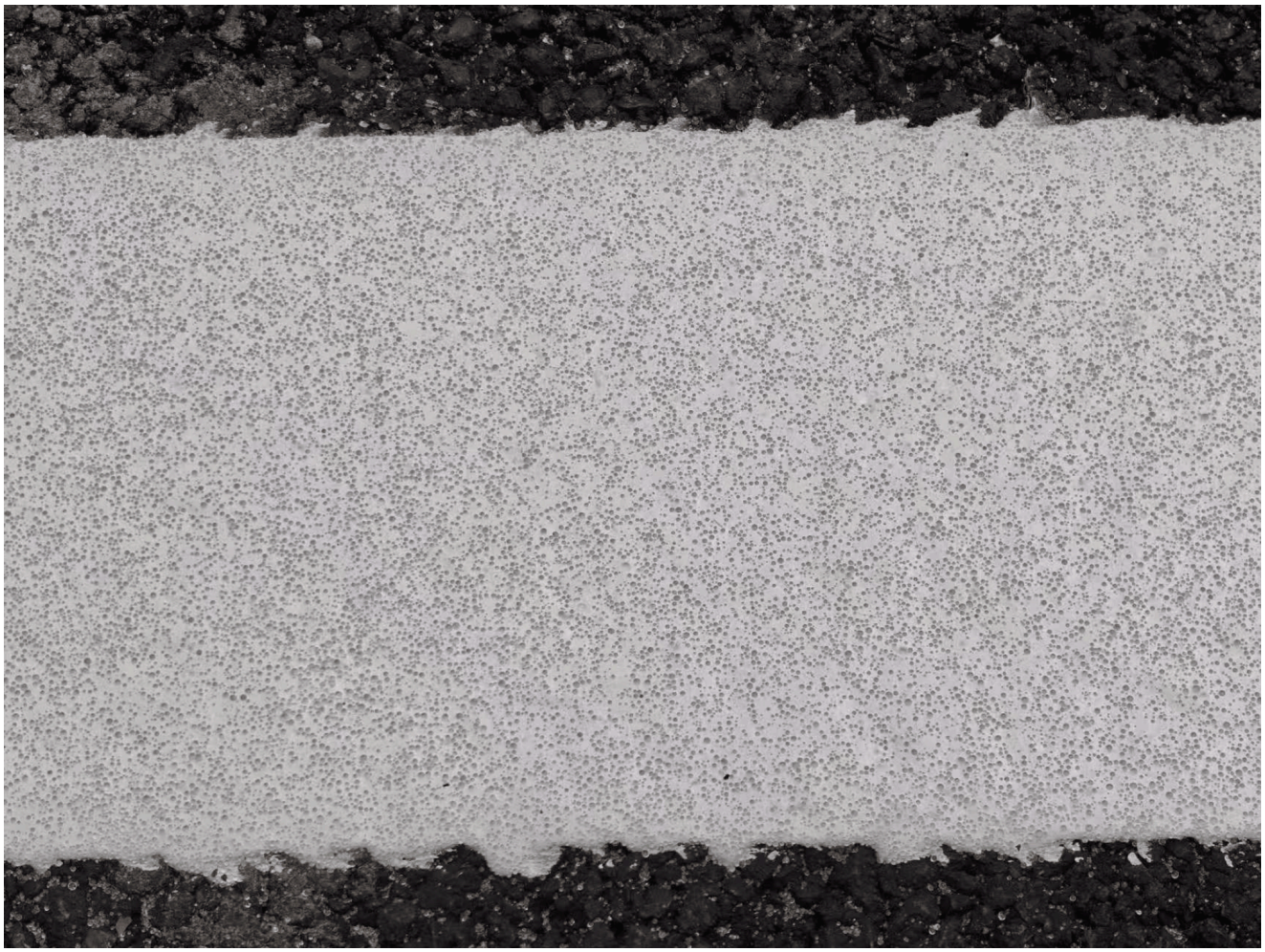


FIGURE 5: Surface of road marking

How to cite this article:
Jiang X (November 17, 2026) Development and Field Performance of a High-Visibility Thermoplastic Road Marking Formulation. Cureus J Eng 3 : es44388-026-00374-2. DOI https://doi.org/10.7759/s44388-026-00374-2

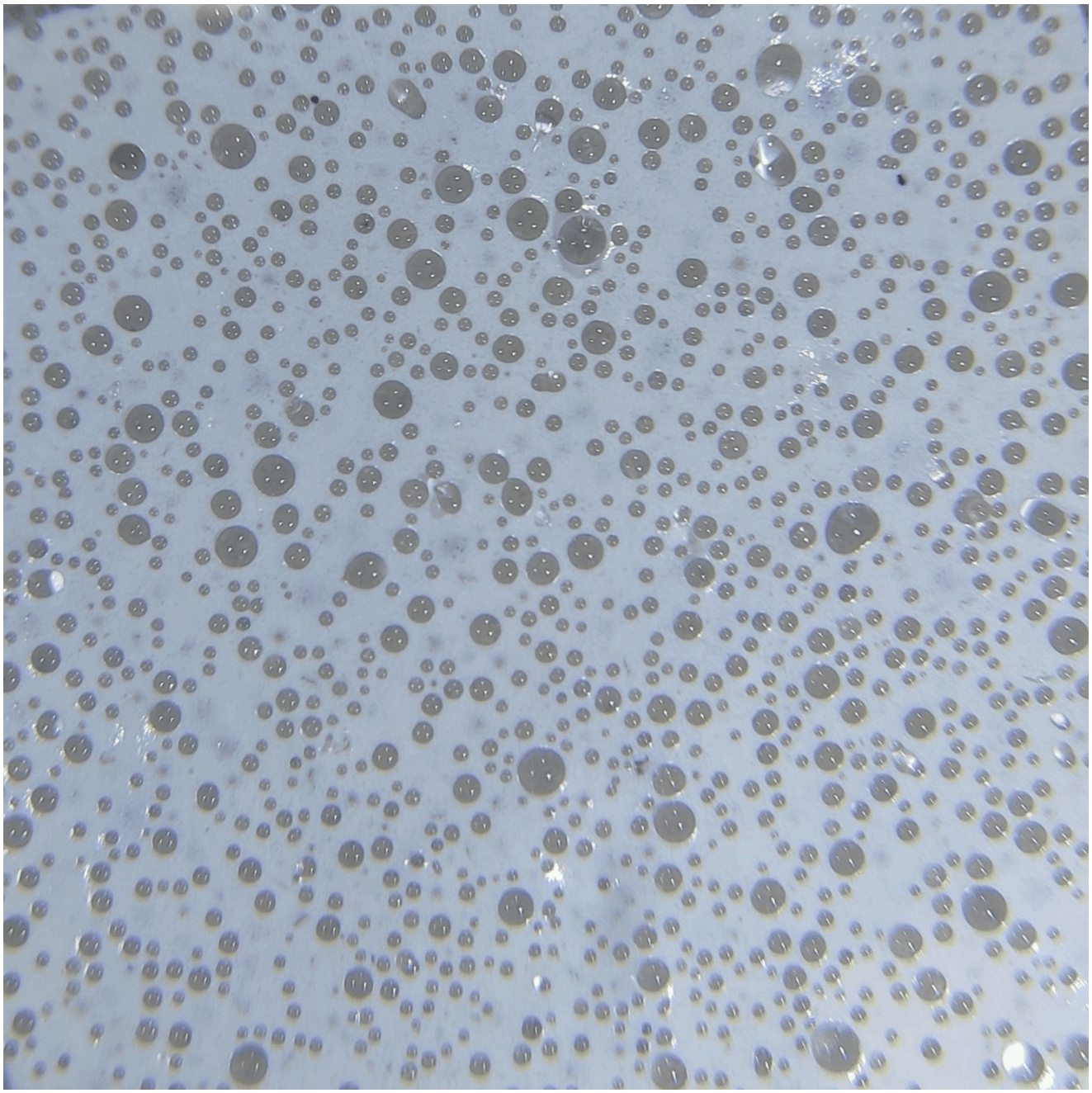


FIGURE 6: Close-up view of drop-on glass beads

Field Measurement and Retroreflectivity Analysis

To objectively evaluate the retroreflective performance of the markings, the detection units and measurement points were meticulously planned according to GB/T 16311-2024, the Chinese national standard for quality requirements and test methods of road traffic markings. This standard specifies the procedures for selecting detection units, laying out test points, and measuring the coefficient of retroreflected luminance. The total length of the tested marking segment was approximately 3 km. Consequently, two distinct 100 m detection units were randomly selected for both the upstream and downstream directions, resulting in four independent detection units in total. Within each unit, 10 test sections were spaced at 10 m intervals.

To account for the distinct traffic patterns on the divided dual-carriageway highway, the 10 test points within each detection unit were distributed across the lanes according to the transverse ratio specified in GB/T 16311-2024: two points on the left edge line, six points on the lane dividing line, and two points on the right edge line. This distribution generated a total of 40 measurement points across the entire test segment. As Figure *7* shows, at each designated point a portable retroreflectometer was utilized to record the luminance coefficient. To minimize instrumental and human error, three repeated measurements were taken per point. Data exhibiting a deviation exceeding 5% from the mean were discarded and the point was re-measured.

The markings were evaluated immediately after construction, at three months, and at six months of service. The field measurement results are summarized in Table *7*.

How to cite this article:
Jiang X (November 17, 2026) Development and Field Performance of a High-Visibility Thermoplastic Road Marking Formulation. Cureus J Eng 3 : es44388-026-00374-2. DOI https://doi.org/10.7759/s44388-026-00374-2



FIGURE 7: Field measurement of retroreflectivity

Marking Position	Initial Retroreflectivity ($mcd \cdot m^{-2} \cdot lx^{-1}$)	3 Months Post-Traffic ($mcd \cdot m^{-2} \cdot lx^{-1}$)	6 Months Post-Traffic ($mcd \cdot m^{-2} \cdot lx^{-1}$)
Left edge line	488	401	336
Lane dividing line	473	407	343
Right edge line	481	399	347
Overall Average	481	402	342

TABLE 7: Field measurement results of retroreflectivity of markings

As demonstrated by the field data, the markings produced with the optimized formulation and the double-drop technique exhibited exceptional initial optical performance. The overall average initial retroreflectivity reached 481 $mcd \cdot m^{-2} \cdot lx^{-1}$, a value that significantly exceeds the national standard requirement of 150 $mcd \cdot m^{-2} \cdot lx^{-1}$ for high-visibility markings. After three months of continuous traffic exposure and environmental weathering, the uppermost floating beads and weakly bonded drop-on beads inevitably wore off. Consequently, the average retroreflectivity decreased to 402 $mcd \cdot m^{-2} \cdot lx^{-1}$, which nevertheless maintained a highly effective level of visibility.

By the sixth month of service, as the uppermost polymer matrix underwent moderate abrasion, the premixed glass beads gradually became exposed and began to function continuously. This transition allowed the average retroreflectivity to stabilize at 342 $mcd \cdot m^{-2} \cdot lx^{-1}$. Furthermore, the degradation trends among the lane dividing lines and the edge lines remained highly consistent, showing no signs of severe localized spalling or optical failure. This remarkable synergistic effect between the drop-on beads and the premixed beads equips the marking with excellent abrasion resistance and sustained retroreflectivity, thereby providing reliable visual guidance for nighttime driving and fully meeting the stringent longevity demands of highways.

Conclusions

Based on systematic parametric optimization and field verification of the thermoplastic road marking materials, the conclusions are as follows. The dosage of premixed glass beads directly governs the wear resistance and high-temperature compressive strength of the coating. Controlling the glass bead content between 31% and 33% facilitates the formation of an optimal anti-wear structural skeleton, which significantly reduces the wear value without compromising the necessary melt flowability during construction. The best overall performance was achieved at 33% glass bead content. The composite filler system is critical for securing both mechanical strength and thermal stability. Incorporating high-hardness quartz sand alongside calcium carbonate creates a robust rigid supporting network. Specifically, setting the quartz sand fraction between 6% and 7% effectively fulfills the rigorous requirement for maintaining compressive strength and deformation resistance at an elevated temperature of 60°C. The optimal balance of these properties was achieved at 6.5% quartz sand content. The enhancement of optical properties by pigment addition exhibits a pronounced marginal effect. Employing structurally stable rutile TiO_2 at a dosage of approximately 5% satisfies all whiteness and luminance factor requirements. Exceeding this threshold yields limited optical improvement and diminishes production cost-effectiveness. The luminance factor reached 83.2% at 5% TiO_2 content, exceeding the standard requirement of 80% without entering the plateau of diminishing returns.

How to cite this article:
Jiang X (November 17, 2026) Development and Field Performance of a High-Visibility Thermoplastic Road Marking Formulation. Cureus J Eng 3 : es44388-026-00374-2. DOI https://doi.org/10.7759/s44388-026-00374-2

Compared to traditional complex multi-additive formulations, the streamlined additive strategy based on DOP and polyethylene wax eliminates phase incompatibility issues while maintaining adequate plasticization and melt rheology. The recommended formulation comprises 31% to 33% premixed glass beads, 6% to 7% quartz sand, 36.5% to 38% calcium carbonate, 4.5% to 5.5% rutile titanium dioxide, 15% to 18% C5 petroleum resin, 0.5% to 1.0% DOP, and 0.5% to 1.5% polyethylene wax. Supported by a rigorous six-month field evaluation conducted in accordance with GB/T 16311-2024, the optimized markings applied with a double-drop bead technique demonstrated exceptional initial retroreflectivity of 481 $mcd \cdot m^{-2} \cdot lx^{-1}$ and outstanding long-term optical retention, with a stabilized value of 342 $mcd \cdot m^{-2} \cdot lx^{-1}$ after six months of traffic exposure. Both values substantially exceed the national standard minimum requirement of 150 $mcd \cdot m^{-2} \cdot lx^{-1}$, confirming that the formulation is highly suitable for demanding highway engineering applications. These findings confirm that careful proportioning of functional components can balance performance and material cost without relying on complex multi-additive systems, providing a practical reference for the formulation design of durable thermoplastic road markings.

Additional Information

Author Contributions

All authors have reviewed the final version to be published and agreed to be accountable for all aspects of the work.

Concept and design: Xiaotian Jiang

Acquisition, analysis, or interpretation of data: Xiaotian Jiang

Drafting of the manuscript: Xiaotian Jiang

Critical review of the manuscript for important intellectual content: Xiaotian Jiang

Disclosures

Human subjects: All authors have confirmed that this study did not involve human participants or tissue.

Animal subjects: All authors have confirmed that this study did not involve animal subjects or tissue.

Conflicts of interest: In compliance with the ICMJE uniform disclosure form, all authors declare the following:

- **Payment/services info:** The research leading to these results has received funding from the Science and technology project of Shuicheng Operation Management Center of Guizhou Expressway Group Co., Ltd. under grant agreement no. SCZX2025092.
- **Financial relationships:** All authors have declared that they have no financial relationships at present or within the previous three years with any organizations that might have an interest in the submitted work.
- **Other relationships:** All authors have declared that there are no other relationships or activities that could appear to have influenced the submitted work.

Data Availability Statements

The datasets (and/or code) supporting this study are available from the corresponding author upon reasonable request.

Acknowledgements

This work was funded by the Science and Technology Project of Shuicheng Operation Management Center, Guizhou Expressway Group Co., Ltd. (Grant No. SCZX2025092), for the project titled "Research and Application of High-Performance Thermoplastic Road Marking Paints".

References

1. Babić D, Fiolić M, Babić D, Gates T: Road markings and their impact on driver behaviour and road safety: A systematic review of current findings. Journal of Advanced Transportation. 2020, 2020:1-19. 10.1155/2020/7843743
2. Kučina I, Kosovec B, Jezidžić F, Ferko M, Babić D: The influence of road marking visibility on lateral vehicle position and driving speed. Acta Polytechnica CTU Proceedings. 2025, 52:69-76. 10.14311/app.2025.52.0069
3. Marciano H: The effect of lane direction pavement markings on driving performance and safety: A driving simulator study. Human Factors. 2024, 66:562-573. 10.1177/00187208221099137
4. Fiolić M, Babić D, Babić D, Tomasović S: Effect of road markings and road signs quality on driving behaviour, driver's gaze patterns and driver's cognitive load at night-time. Transportation Research Part F: Traffic Psychology and Behaviour. 2023, 99:306-318. 10.1016/j.trf.2023.10.025
5. Ariën C, Brijs K, Vanroelen G, et al.: The effect of pavement markings on driving behaviour in curves: a simulator study. Ergonomics. 2017, 60:701-713. 10.1080/00140139.2016.1200749
6. Babić D, Burghardt TE, Babić D: Application and characteristics of waterborne road marking paint. International Journal for Traffic and Transport Engineering. 2015, 5:150-169. 10.7708/ijtte.2015.5(2).06
7. Naidu V, Bhaiswar V: Review on road marking paint machine and material. IOP Conference Series: Materials Science and Engineering. 2020, 954:012016. 10.1088/1757-899x/954/1/012016
8. Xu L, Chen Z, Li X, Xiao F: Performance, environmental impact and cost analysis of marking materials in pavement engineering, the-state-of-art. Journal of Cleaner Production. 2021, 294:126302. 10.1016/j.jclepro.2021.126302
9. Obeng DA, Owusu V, Tuffour YA: Degradation of retro-reflectivity of thermoplastic pavement markings on trunk roads in Ghana. Transportation Engineering. 2021, 5:100082. 10.1016/j.treng.2021.100082
10. Zhao L, Ding H, Sun J, Wu G, Xing H, Wang W, Song J: Prediction of service life of thermoplastic road markings on expressways. Sustainability. 2023, 15:15237. 10.3390/su152115237
11. Quan X, Yang L, Li H, Chen Y, Shi S: Performance evaluation of a multifunctional road marking coating for tunnels based on Nano SiO2 and TiO2 modifications. Buildings. 2024, 14:459. 10.3390/buildings14020459
12. Wang J, Song S, Li Q, Zhang L, Wang N: The effect of glass beads sizes and surface treatment on the bonding performance of asphalt pavement marking. Case Studies in Construction Materials. 2025, 22:e04882. 10.1016/j.cscm.2025.e04882
13. Eren E, Mypati VNK, Praticò FG: Energy and surface performance of light-coloured surface treatments. Sustainability. 2025, 17:8902. 10.3390/su17198902
14. Lu J, Zhang M, Feng J, Gao Y, Yang Y, Li Y, Li L: Investigation on the technical performance and workability of hot-melting road marking materials using for the high-altitude area. Case Studies in Construction Materials. 2023, 18:e02027. 10.1016/j.cscm.2023.e02027
15. Mirabedini SM, Jamali SS, Haghayegh M, Sharifi M, Mirabedini AS, Hashemi-Nasab R: Application of mixture experimental design to optimize formulation and performance of thermoplastic road markings. Progress in Organic Coatings. 2012, 75:549-559. 10.1016/j.porgcoat.2012.05.012
16. Burghardt T, Pashkevich A: Materials selection for structured horizontal road markings: financial and environmental case studies. European Transport Research Review. 2020, 12:1-10. 10.1186/s12544-020-0397-x
17. Kohnechi P, Fasihi M, Eshaghi H: Rheology, mechanical properties and peel adhesion of hot-melt adhesive based on thermoplastic polyurethane/nanosilica. International Journal of Adhesion and Adhesives. 2023, 125:103440. 10.1016/j.ijadhadh.2023.103440
18. Allen NS, Edge M, Ortega A, et al.: Behaviour of nanoparticle (ultrafine) titanium dioxide pigments and stabilisers on the photooxidative stability of water based acrylic and isocyanate based acrylic coatings. Polymer Degradation and Stability. 2002, 78:467-478. 10.1016/s0141-3910(02)00189-1
19. Li K, Peng J, Zhang M, et al.: Comparative study of the effects of anatase and rutile titanium dioxide nanoparticles on the structure and properties of waterborne polyurethane. Colloids and Surfaces A: Physicochemical and Engineering Aspects. 2015, 470:92-99. 10.1016/j.colsurfa.2015.01.072
20. Bek M, Gonzalez-Gutierrez J, Kukla C, et al.: Rheological behaviour of highly filled materials for injection moulding and additive manufacturing: effect of particle material and loading. Applied Sciences. 2020, 10:7993. 10.3390/app10227993

How to cite this article:
Jiang X (November 17, 2026) Development and Field Performance of a High-Visibility Thermoplastic Road Marking Formulation. Cureus J Eng 3 : es44388-026-00374-2. DOI https://doi.org/10.7759/s44388-026-00374-2

21. Behl S, Farahani AD, Raju, et al.: Evaluation of rheological behaviour of flowable dental composites reinforced with low aspect ratio micro-sized glass fibres. Dental Materials. 2021, 37:131-142. 10.1016/j.dental.2020.10.023

How to cite this article:
Jiang X (November 17, 2026) Development and Field Performance of a High-Visibility Thermoplastic Road Marking Formulation. Cureus J Eng 3 : es44388-026-00374-2. DOI https://doi.org/10.7759/s44388-026-00374-2